Supporting Information

High-efficiency photoelectrocatalytic oxygen evolution reaction enabled by MXene-derived TiO_2 coupled with FeP nanoparticles

Hengjun Su,[a,#] Xiaojun Zeng,[a,#,*] Liangqi Gui,[a] Huiqin Zhao,[a] Xiaofeng Zhang[b,*]

[a] Jiangxi Key Laboratory of Advanced Ceramic Materials, School of Materials Science and Engineering, Jingdezhen Ceramic University, Jingdezhen 333403, China

[b] Guangdong Academy of Science, Guangdong Institute of New Materials, National Engineering Laboratory for Modern Materials Surface Engineering Technology, The Key Lab of Guangdong for Modern Surface Engineering Technology, Guangzhou 510650, China

* Corresponding author, E-mail: zengxiaojun@jcu.edu.cn (X.J. Zeng), zxf200808@126.com (X.F. Zhang)

[#] These authors contributed equally to this work.

The turnover frequency (TOF), mass activity and specific activity are calculated according to the following Equations 1, 2, and 3, respectively.[1-3]

$$\text{TOF} = jS/(4Fn) \quad (1)$$

$$\text{Mass activity} = j/m \quad (2)$$

$$\text{Specific activity} = j/(10m\,S_{\text{BET}}) \quad (3)$$

where j (mA cm^{-2}) is the measured current density at overpotential η = 0.30 V, m (mg cm^{-2}) is the loading density of catalyst on the electrode, S_{BET} (m^2 g^{-1}) is the BET specific surface area, S (0.196 cm^2) is the surface area of the GCE, F (96485 C mol^{-1}) is the Faraday constant, the number of 4 means four electrons per O_2 molecule, and n is the total molar number of metal ions calculated according to the loading density of catalyst.

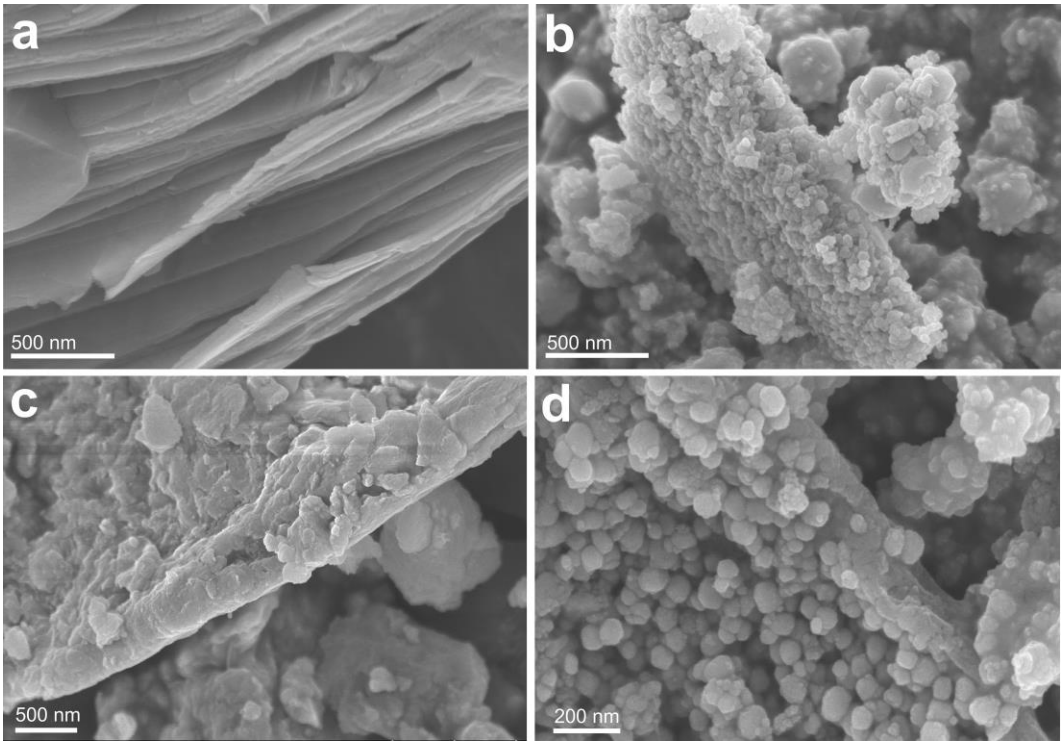

Figure S1. SEM images of (a) MXene, (b) MXene/FeP, (c) MXene@TiO_2, and (d) MXene@TiO_2/FeP.

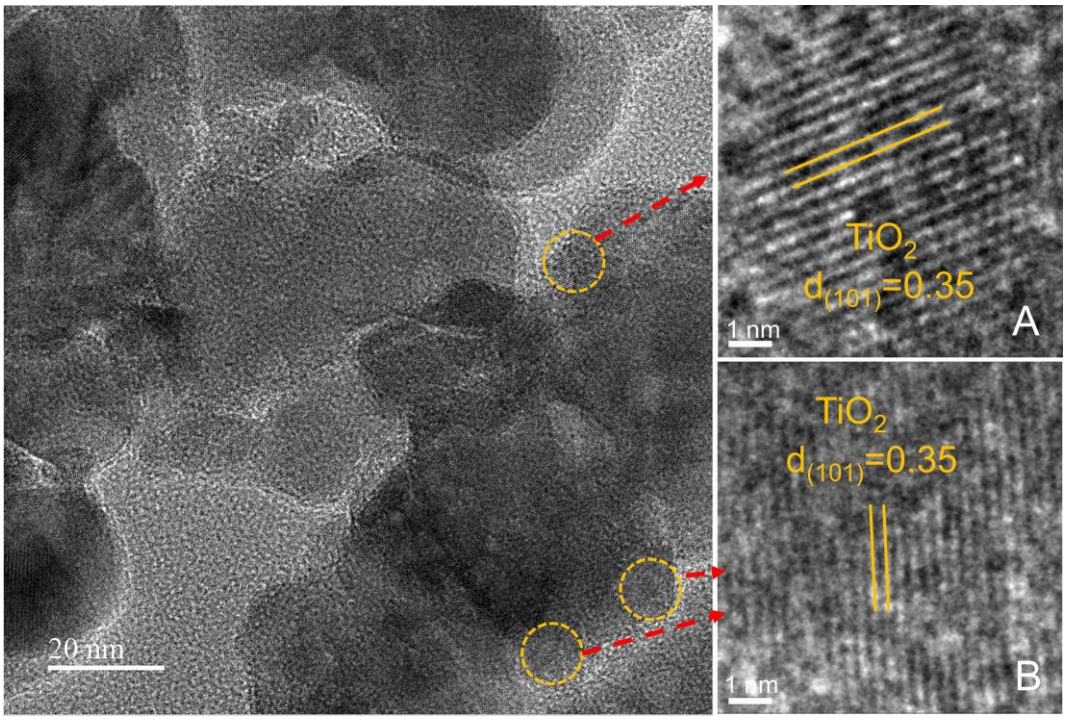

Figure S2. HRTEM image of MXene@TiO_2/FeP.

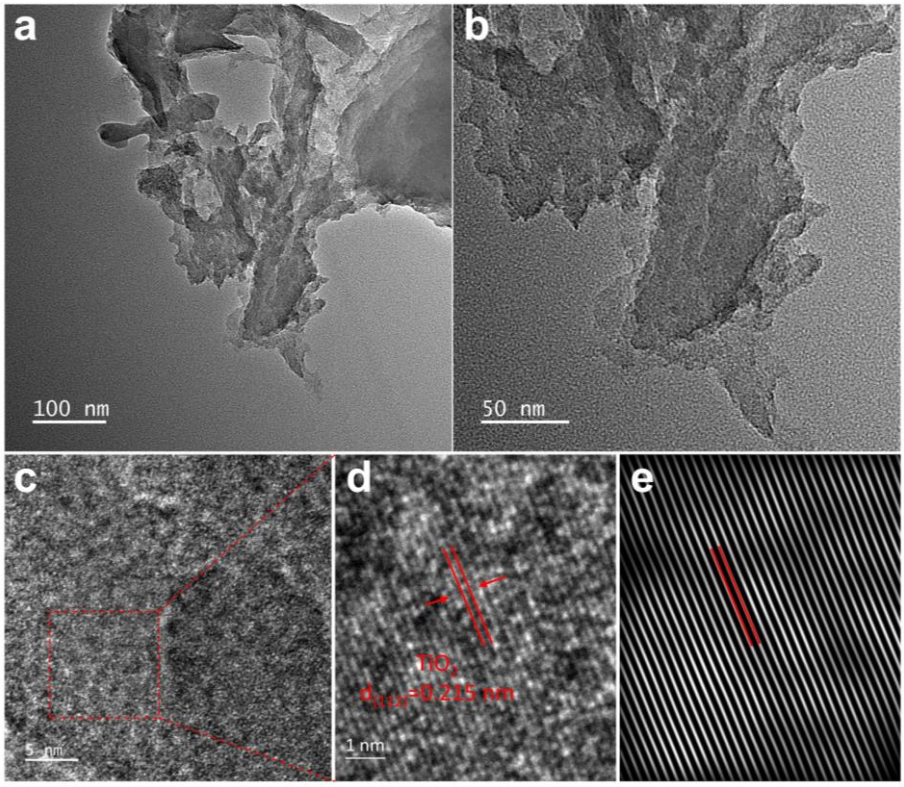

Figure S3. (a,b) TEM and (c-e) HRTEM images of MXene@TiO_2.

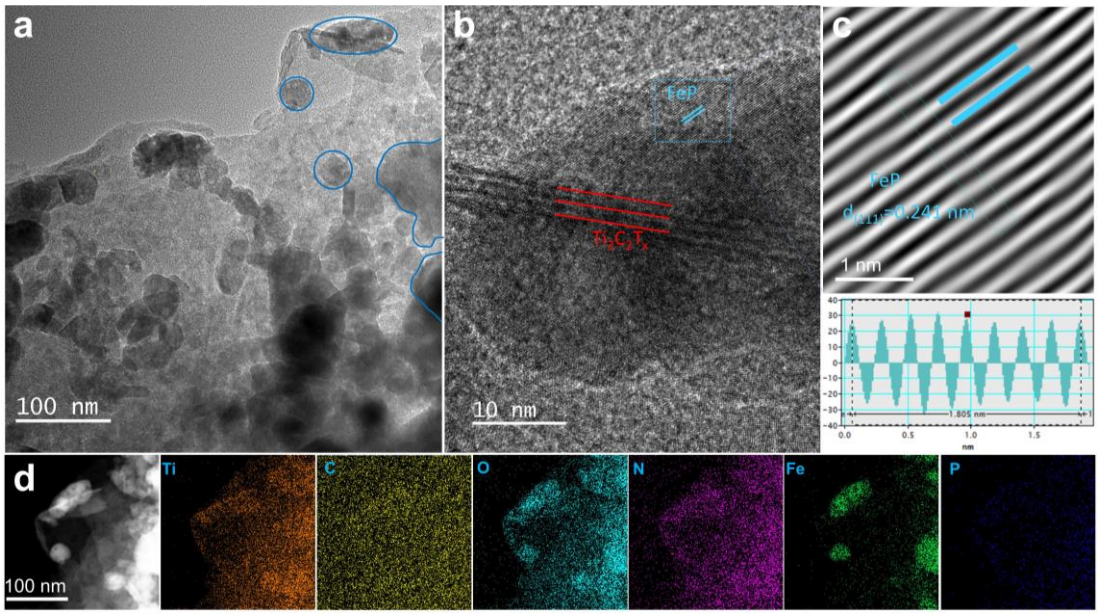

Figure S4. (a) TEM and (b,c) HRTEM images of MXene/FeP. (d) Elemental mapping images of MXene/FeP.

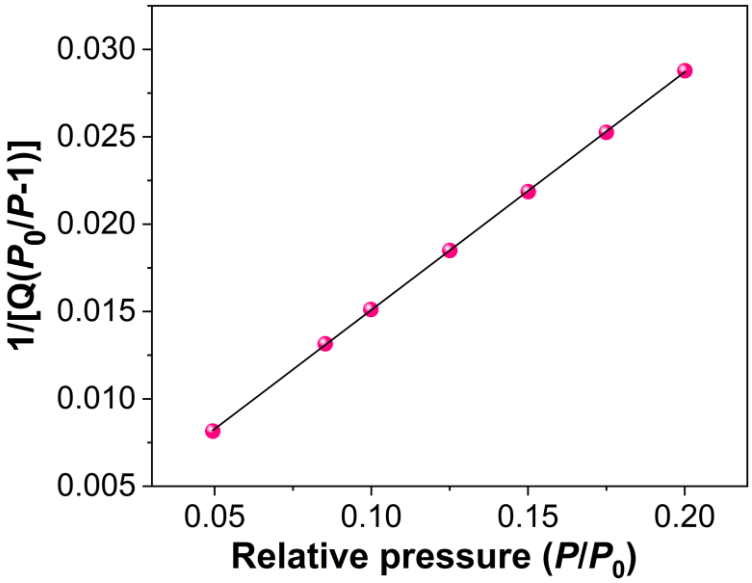

Figure S5. BET surface area plot of MXene@TiO_2/FeP.

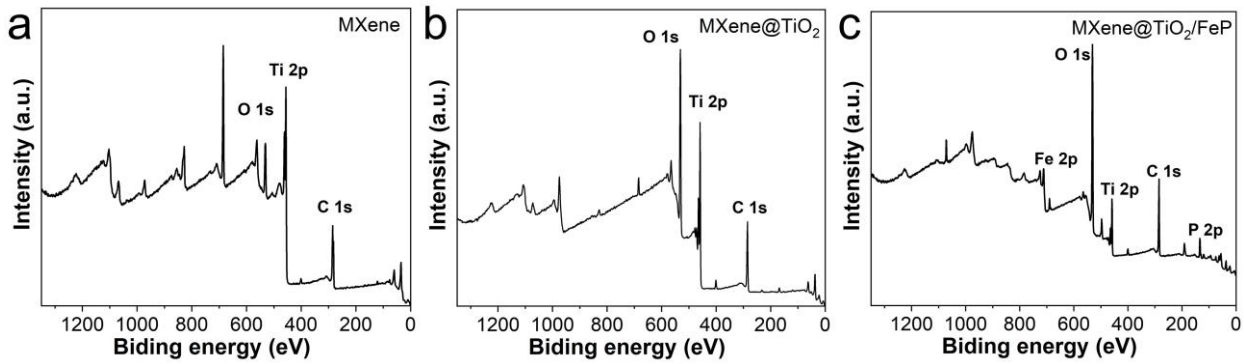

Figure S6. XPS survey spectra of (a) MXene, (b) MXene@TiO_2, and (c) MXene@TiO_2/FeP.

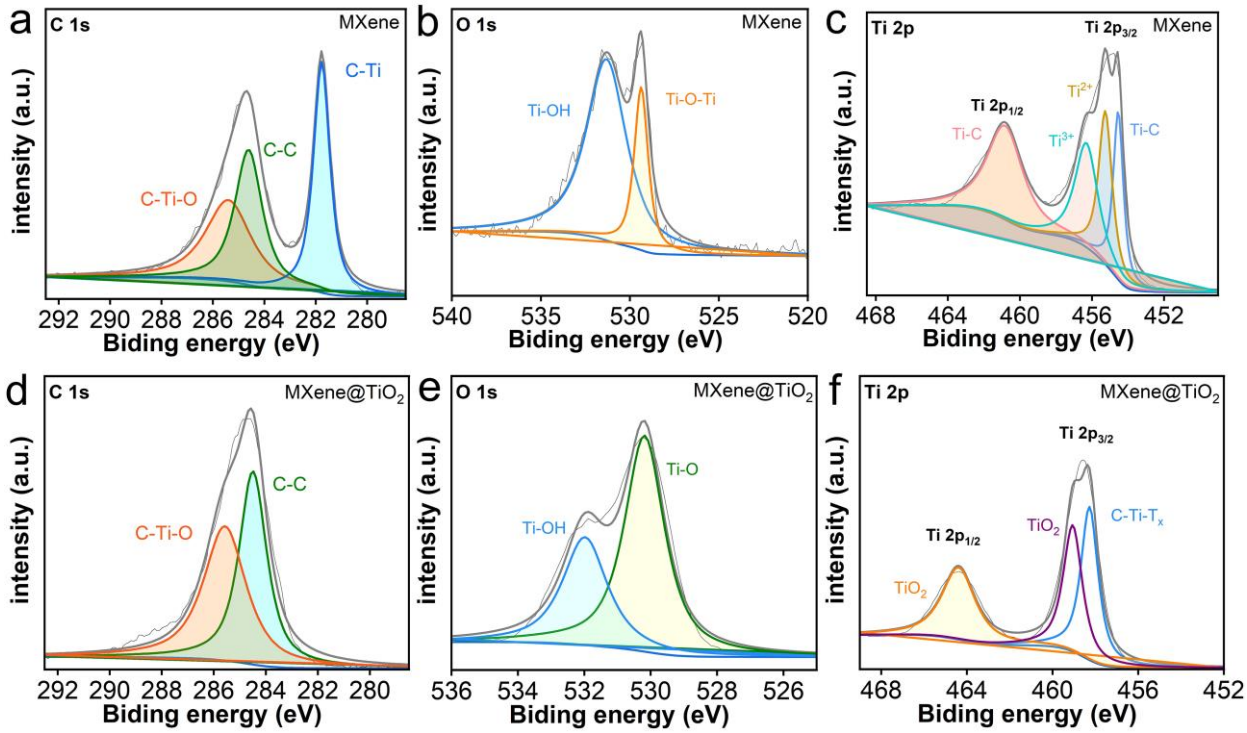

Figure S7. High-resolution XPS spectra of (a,d) C 1s, (b,e) O 1s, and (c,f) Ti 2p for (a-c) MXene and (d-f) MXene@TiO_2.

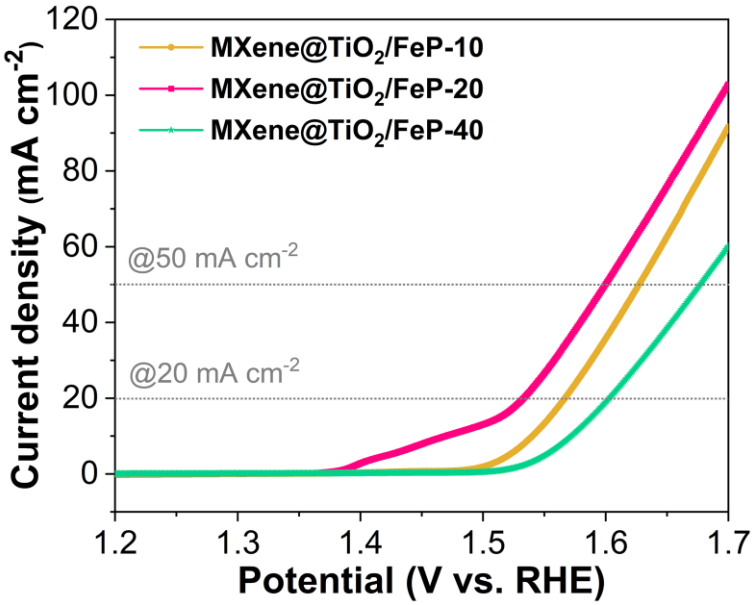

Figure S8. LSV curves of MXene@TiO_2/FeP with 10, 20, and 40 mg of MXene@TiO_2.

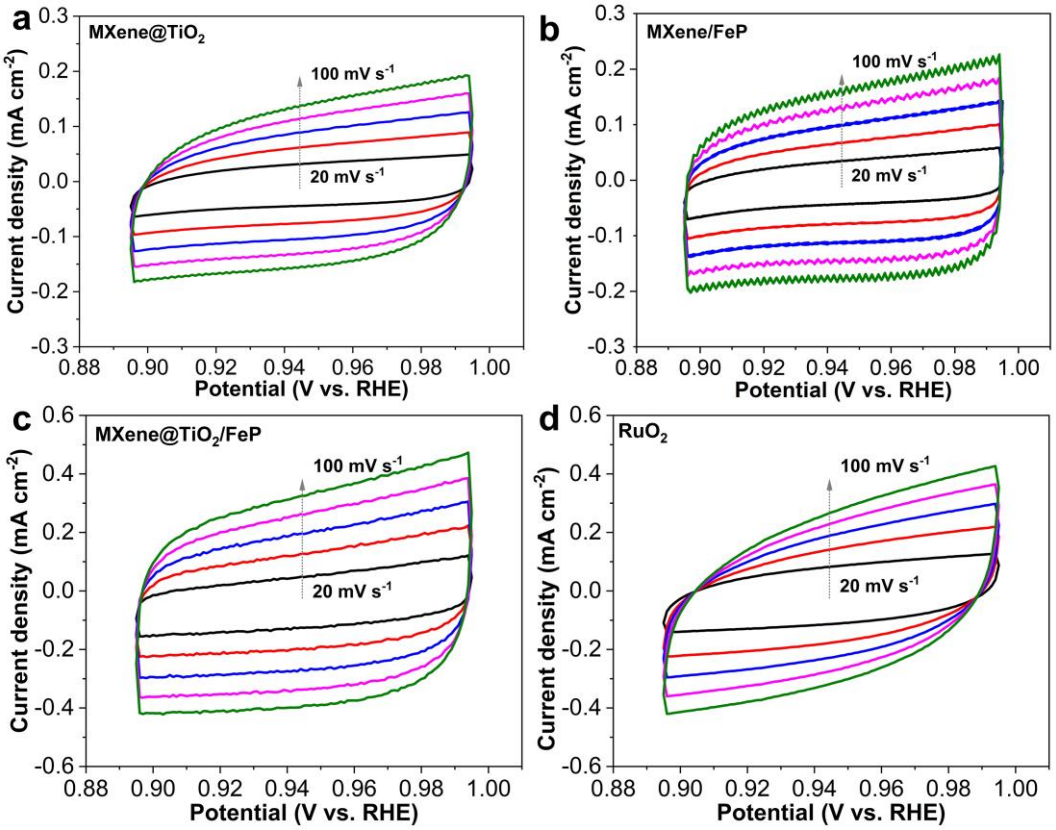

Figure S9. CV curves of (a) MXene@TiO_2, (b) MXene/FeP, (c) MXene@TiO_2/FeP, and (d) RuO_2 catalysts at different scan rates of 20~100 mV s^{-1}.

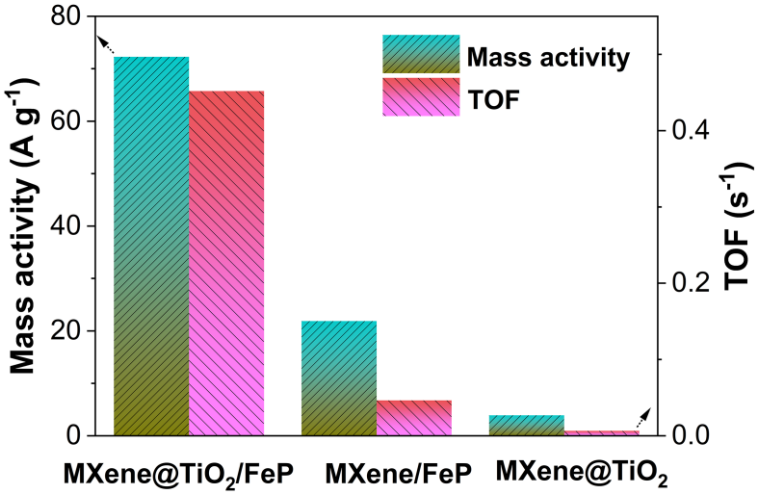

Figure S10. TOF and mass activity of the samples.

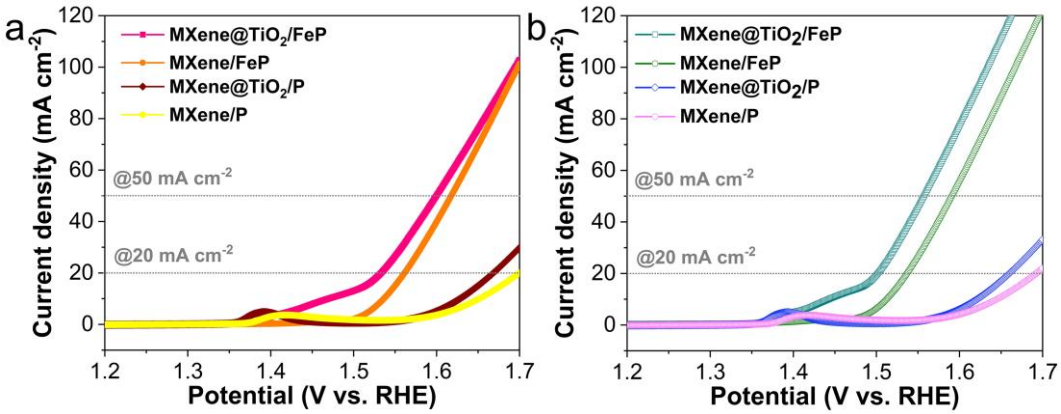

Figure S11. LSV curves of MXene@TiO_2/FeP, MXene/FeP, MXene/P, and MXene@TiO_2/P catalysts under (a) dark and (b) light conditions.

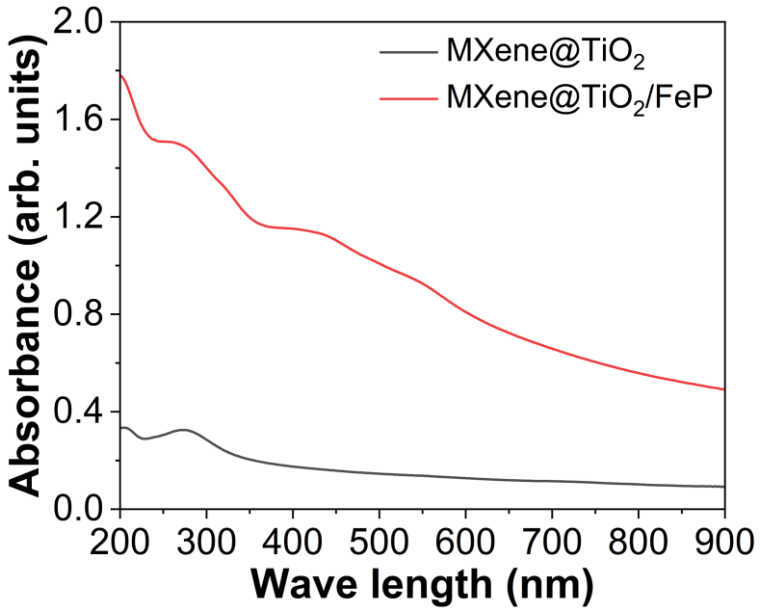

Figure S12. UV-visible absorption spectra of MXene@TiO_2 and MXene@TiO_2/FeP.

Table S1. TOF of the samples at overpotential of 300 mV.

Samples	$m_{catalyst}$ (mg)	Loading mass (mg cm^{-2})	M (g mol^{-1})	n (mol)	TOF (s^{-1})
MXene@TiO_2/FeP	2.92	0.5615	289.44	0.00194	0.2780
MXene/FeP	4.08	0.6022	209.57	0.00287	0.1694
MXene@TiO_2	4.52	0.7629	122.75	0.00621	0.0165

Table S2. Mass activities of the samples.

Samples	Loading mass (mg)	*j* (mA cm^{-2})	Mass activity (A g^{-1})
MXene@TiO_2/FeP	2.92	40.033	71.29164384
MXene/FeP	4.08	27.73	46.04675245
MXene@TiO_2	4.52	6.667	8.739375

Table S3. Comparison of OER performance between MXene@TiO_2/FeP and reported MXene-based OER electrocatalysts.

Electrocatalysts	Electrolyte	Overpotential (mV)	Loading (mg cm^{-2})	References
CoP/Mo_2CT_x	1 M KOH	260	0.40	[4]
NiFeMnCoP/MXene	1 M KOH	240	0.24	[5]
Ti_3C_2@mNiCoP	1 M KOH	237	2.00	[6]
NiFeCoP/Ti_3C_2	1 M KOH	240	0.60	[7]
NiFeP/MXene	1 M KOH	286	0.25	[8]
CoP@3D Ti_3C_2	1 M KOH	220	0.20	[9]
CoP/MXene	1 M KOH	230	1.50	[10]
CoP/Ti_3C_2 MXene	1 M KOH	280	0.13	[11]
$Ni_{0.7}Fe_{0.3}PS_3$@MXene	1 M KOH	282	0.25	[12]
CoNi/CoNiP/MXene	0.1 M KOH	294	0.25	[13]
MXene@TiO_2/FeP	1 M KOH	240	0.55	This work

Table S4. Photo-electrochemical OER performance of the samples.

Samples	Off light irradiation (mV)	On Light irradiation (mV)	Change value (mV)
MXene@TiO_2/FeP	244	213	31
MXene/FeP	311.7	318.2	6.5
MXene@TiO_2	391	374	17
FeP	288	288	0
MXene/P	422	414.8	7.2
MXene@TiO_2/P	415	391	24
MXene@TiO_2Fe/P-10	317.3	304.2	13.1
MXene@TiO_2Fe/P-40	343.7	294.6	49.1

References

[1] Y. X. Li, J. Yin, L. An, M. Lu, K. Sun, Y.-Q. Zhao, D. Q. Gao, F. Y. Cheng, P. X. Xi, FeS_2/CoS_2 interface nanosheets as efficient bifunctional electrocatalyst for overall water splitting, *Small*, 2018, **14**, 1801070.

[2] X. Y. Yue , C. S. Song, Z. Y. Yan, X. P. Shen, W. T. Ke, Z. Y. Ji, G. X. Zhu, A. H. Yuan, J. Zhu, B. L. Li. Reduced graphene oxide supported nitrogen-doped porous carbon-coated NiFe alloy composite with excellent electrocatalytic activity for oxygen evolution reaction, *Appl. Surf. Sci.*, 2019, **493**, 963-974.

[3] L. Wu, X. P. Shen, Z. Y. Ji, J. R. Yuan, S. K. Yang, G. X. Zhu, L. Z. Chen, L. R. Kong, H. B. Zhou. Facile synthesis of medium-entropy metal sulfides as high-efficiency electrocatalysts toward oxygen evolution reaction, *Adv. Funct. Mater.*, 2023, **33**, 2208170.

[4] S. H. Liu, Z. S. Lin, R. D. Wan, Y. Liu, Z. Liu, S. D. Zhang, X. F. Zhang, Z. H. Tang, X. X.

Lu, Y. Tian, Cobalt phosphide supported by two-dimensional molybdenum carbide (MXene) for the hydrogen evolution reaction, oxygen evolution reaction, and overall water splitting, *J. Mater. Chem. A*, 2021, **9**(37), 21259-21269.

[5] L. H. Liu, N. Li, J. R. Han, K. L. Yao, H. Y. Liang, Multicomponent transition metal phosphide for oxygen evolution, *Int. J. Min. Met. Mater.*, 2022, **29**(3), 503-512.

[6] Q. Yue, J. Sun, S. Chen, Y. Zhou, H. J. Li, Y. Chen, R. Y. Zhang, G. F. Wei, Y. J. Kang, Hierarchical mesoporous MXene-NiCoP electrocatalyst for water-splitting, *ACS Appl. Mater. Interfaces*, 2020, **12**(16), 18570-18577.

[7] N. Li, J. R. Han, K. L. Yao, M. Han, Z. M. Wang, Y. C. Liu, L. H. Liu, H. Y. Liang, Synergistic phosphorized NiFeCo and MXene interaction inspired the formation of high-valence metal sites for efficient oxygen evolution, *J. Mater. Sci. Technol.*, 2022, **106,** 90-97.

[8] J. X. Chen, Q. W. Long, K. Xiao, T. Ouyang, N. Li, S. Y. Ye, Z. Q. Liu, Vertically-interlaced NiFeP/MXene electrocatalyst with tunable electronic structure for high-efficiency oxygen evolution reaction, *Sci. Bull.*, 2021, **66**(11), 1063-1072.

[9] L. Y. Xiu, Z. Y. Wang, M. Z. Yu, X. H. Wu, J. S. Qiu, Aggregation-resistant 3D MXene-based architecture as efficient bifunctional electrocatalyst for overall water splitting, *ACS Nano*, 2018, **12**(8), 8017-8028.

[10] N. C. S. Selvam, J. Lee, G. H. Choi, M. J. Oh, S. Y. Xu, B. Lim, P. J. Yoo, MXene supported Co_xA_y (A= OH, P, Se) electrocatalysts for overall water splitting: unveiling the role of anions in intrinsic activity and stability, *J. Materi. Chem. A*, 2019, **7**(48), 27383-27393.

[11] L. Yan, B. Zhang, S. Y. Wu, J. L. Yu, A general approach to the synthesis of transition metal phosphide nanoarrays on MXene nanosheets for pH-universal hydrogen evolution and alkaline overall water splitting, *J. Mater. Chem. A*, 2020, **8**(28), 14234-14242.

[12] C. F. Du, K. N. Dinh, Q. H. Liang, Y. Zheng, Y. B. Luo, J. L. Zhang, Q. Y. Yan, Self-assemble and in situ formation of $Ni_{1-x}Fe_xPS_3$ nanomosaic-decorated MXene hybrids for overall

water splitting, *Adv. Energy Mater.*, 2018, **8**(26), 1801127.

[13] J. Y. Qiao, Z. H. Bao, L. Q. Kong, X. Y. Liu, C. J. Lu, M. Ni, W. He, M. Zhou, Z. M. Sun, MOF-derived heterostructure CoNi/CoNiP anchored on MXene framework as a superior bifunctional electrocatalyst for zinc-air batteries, *Chinese Chem. Lett.*, 2023, **34**(12), 108318.